

Superfluid nuclear matter calculations

P. Bozek*

National Superconducting Cyclotron Laboratory,
and Department of Physics and Astronomy,
Michigan State University, East Lansing, MI-48824
and

Institute of Nuclear Physics, PL-31-342 Kraków, Poland

September 10, 2018

Abstract

We present a method to calculate nuclear matter properties in the superfluid phase. The method is based on the use of self-consistent off-shell nucleon propagators in the T-matrix equation. Such a complete treatment of the spectral function, is required below and around T_c due to a pseudogap formation in the spectral function. In the superfluid phase we introduce the anomalous self-energy in the fermion propagators and in the T-matrix equation, consistently with the strong coupling BCS equations. The equations for the nucleon spectral function include both a contribution of condensed and scattering pairs. The method is illustrated by numerical calculations. Above T_c pseudogap formation is visible in the spectral function and below T_c a superfluid gap also appears.

PACS: 24.10Cn, 21.65+f

Keywords: Nuclear matter, superfluidity, spectral function

*electronic address : bozek@solaris.ifj.edu.pl

1 Introduction

Nuclear matter calculations in the Brueckner approximation [1, 2] do not consider a possible pairing in the ground state of nuclear matter [3], with the exception of Refs. [4]. This approach is justified by the fact that the superfluid energy gap is expected to be small in normal density nuclear matter [2]. When addressing the spectral properties of nucleons in medium, calculations using T-matrix approximation were performed [5, 6, 7, 8]. The T-matrix approximation for the two-particle Green's functions leads to a much stronger pairing than the Brueckner approximation. The T-matrix calculation and the BCS theory give the same prediction for the critical temperature [9]. Brueckner type calculations of the effective in-medium nuclear interactions, permit to estimate approximate nuclear matter ground state energy, in-medium nucleon masses, and effective cross sections from the free nucleon-nucleon interaction. Although, discrepancies between different calculations and different parameterization of the nuclear interaction remain, a tremendous improvement over a simple Hartree-Fock approach is achieved. It is an interesting question, how to include the pairing force into this picture.

The generalization of the T-matrix nuclear matter calculations below the superfluid transition temperature (T_c), requires by itself a procedure combining the ladder summation of the self-energy diagrams and a possible fermion pairing. On the other hand, the T-matrix scheme seems to be a natural starting point for the inclusion of superfluidity in nuclear matter calculations [9, 10]. In this work we show that such a procedure is indeed possible, merging a T-matrix calculation of the normal fermion self-energy with a mean-field, frequency independent, superfluid energy gap. The interaction potential, which enters in the superfluid gap equation is the free nucleon-nucleon interaction. However, the scattering of nucleons and the pseudogap formation above the critical temperature reduces the value of the energy gap and of the critical temperature, as compared to the BCS result. This can be achieved only using self-consistent off-shell propagators in the T-matrix diagrams [11]. In such a way the formation of a pseudogap influences strongly the result for the T-matrix in attractive channels, shifting the appearance of a singularity in the T-matrix

at the Fermi energy to much lower temperatures. A consistent treatment of the superfluid transition requires then both the use of the off-shell nucleon propagators (below and above T_c) and of the anomalous self-energy (below T_c). To illustrate the formation of the pseudogap above T_c , we present first the results of two calculations above T_c (Sec. 3), a self-consistent T-matrix resummation, using off-shell propagators and a T-matrix calculation using on-shell nucleon propagators with Hartree-Fock single-particle energies. The results of that section indicate the necessity of using off-shell propagators in the T-matrix equation around T_c , rather than a quasi-particle approximation. In section 4 we derive the equation for the T-matrix self-energy and the gap equations, in the superfluid phase. A numerical example of a self-consistent calculation of the superfluid energy gap and of the T-matrix self-energy is presented in section 5.

2 T-matrix equation in the Fermi liquid phase

The nuclear matter can be described as an infinite system of interacting fermions. We consider a system of neutrons and protons interacting via two-body forces

$$H = \sum_{\alpha} \int d^3x \Psi_{\alpha}^{\dagger}(x) \left(-\frac{\Delta^2}{2m} - \mu \right) \Psi_{\alpha}(x) + \sum_{\alpha', \beta', \alpha, \beta} \frac{1}{2} \int d^3x \int d^3y \Psi_{\alpha'}^{\dagger}(x) \Psi_{\beta'}^{\dagger}(y) V_{\alpha', \beta', \alpha, \beta}(x, y) \Psi_{\beta}(y) \Psi_{\alpha}(x) . \quad (1)$$

Note that we define the energies with respect to the Fermi energy (chemical potential) μ ; also for real-time calculations. This will be helpful when dealing with the anomalous propagator in the superfluid phase. In the following we shall use equivalently the term zero energy and the Fermi energy. Nuclear forces can be decomposed in (JST) (total angular-momentum, spin, isospin) channels [13]

$$V_{\alpha', \beta', \alpha, \beta}(\mathbf{k}, \mathbf{p}) = \sum_{(JST)ll'} i^{l-l'} \mathcal{Y}_{\alpha' \beta'}^{(JST)l}(\hat{k}) V_{ll'}^{(JST)}(k, p) \mathcal{Y}_{\alpha \beta}^{(JST)l'}(\hat{p})^* . \quad (2)$$

The sum over the partial waves l, l' is restricted to $l = l' = J$ for uncoupled states and to $l, l' = J \pm 1$ for the scattering of triplet states.

One body observables of a system of fermions at equilibrium can be described by the spectral function

$$A(p, \omega) = -2\text{Im}G^+(p, \omega) = \frac{-2\text{Im}\Sigma^+(p, \omega)}{(\omega - p^2/2m - \text{Re}\Sigma^+(p, \omega) + \mu)^2 + \text{Im}\Sigma^+(p, \omega)^2} , \quad (3)$$

where G^{\pm} denote the retarded(advanced) Green's function. We restrict the discussion to symmetric nuclear matter so that the Green's function is diagonal in spin-isospin indices. The T-matrix approximation consists of summing particle-particle and hole-hole ladder diagrams for the self-energy [14, 15, 16]. The self-energy for in-medium propagators describes the dressing of the quasi-particles due to scatterings with other particles. In general one cannot approximate the spectral function by a δ -function (quasi-particle peak) at some quasi-particle energy ζ_k . The particles acquire a width, which enters self-consistently in the equation for the T-matrix. Moreover, more complicated structures in the spectral function seem to appear when the temperature is in a range of few MeV above the superfluid transition [8]. Using a quasiparticle ansatz for the spectral function the authors of Ref. [8] have shown that the spectral function has two (or sometimes three) peaks. This effect by itself invalidates the quasi-particle approximation for the T-matrix. On the other hand, it is possible to calculate the T-matrix and the corresponding spectral function self-consistently using off-shell propagators in the ladder diagrams for the self-energy [11]. The self-consistent calculation was performed in a simple model with separable interactions in the S -wave. In the present work we use this simple interaction for numerical examples. The self-consistent solution encompasses in a consistent way the non-Fermi liquid behavior of the spectral functions, and, thus, gives quantitatively different results for the critical temperature and for the temperature where the pseudogap appears, than the quasi-particle approximation.

Off-shell propagators were used previously in a nuclear matter calculation by Jong and Lenske [12]. The spectral function in that work was approximated as a sum of a quasiparticle peak and a continuum part on the other side of the Fermi energy, the contribution to the two particle propagator with two continuum

spectral functions was neglected to simplify the numerics. This neglected part could be calculated using the methods developed in the present work. On the other hand a mixed ansatz using a quasi-particle and a continuum part for the spectral function, like the one used in [12] or similar, is unavoidable at small temperatures. The authors of Ref [12] use a self-consistent scheme a zero temperature, but do not consider pairing. However, even if the expected pairing is small it is more natural to use a scheme allowing for the creation of pair condensate, since the normal Fermi liquid is unstable.

The T-matrix for a system with a two-body interaction $V(\mathbf{p}, \mathbf{p}')$ is defined as [14, 15, 16, 17] :

$$\begin{aligned} \langle \mathbf{p} | T_{\alpha' \beta' \alpha \beta}^{\pm}(\mathbf{P}, \omega) | \mathbf{p}' \rangle &= V_{\alpha' \beta' \alpha \beta}(\mathbf{p}, \mathbf{p}') \\ &+ \sum_{\gamma \delta} \int \frac{d^3 k}{(2\pi)^3} \int \frac{d^3 q}{(2\pi)^3} V_{\alpha' \beta' \gamma \delta}(\mathbf{p}, \mathbf{k}) \\ &\langle \mathbf{k} | \mathcal{G}^{\pm}(\mathbf{P}, \omega) | \mathbf{q} \rangle \langle \mathbf{q} | T_{\gamma \delta \alpha \beta}^{\pm}(\mathbf{P}, \omega) | \mathbf{p}' \rangle , \end{aligned} \quad (4)$$

where the disconnected two-particle propagator is :

$$\begin{aligned} \langle \mathbf{p} | \mathcal{G}^{\pm}(\mathbf{P}, \omega) | \mathbf{p}' \rangle &= (2\pi)^3 \delta^3(\mathbf{p} - \mathbf{p}') \int \frac{d\omega'}{2\pi} \int \frac{d\omega''}{2\pi} \\ &\left(G^<(\mathbf{P}/2 + \mathbf{p}, \omega'' - \omega') G^<(\mathbf{P}/2 - \mathbf{p}, \omega') \right. \\ &\left. - G^>(\mathbf{P}/2 + \mathbf{p}, \omega'' - \omega') G^>(\mathbf{P}/2 - \mathbf{p}, \omega') \right) / \left(\omega - \omega'' \pm i\epsilon \right) , \end{aligned} \quad (5)$$

with

$$\begin{aligned} G^<(p, \omega) &= iA(p, \omega)f(\omega) \\ G^>(p, \omega) &= -iA(p, \omega)\left(1 - f(\omega)\right) , \end{aligned} \quad (6)$$

and

$$f(\omega) = \frac{1}{e^{\omega/T} + 1} \quad (7)$$

is the Fermi distribution. The in-medium T-matrix equation can be decomposed in partial waves if an angle averaged two-particle propagator $\langle \mathcal{G} \rangle_{\Omega}$ is used :

$$\langle \langle \mathbf{p} | \mathcal{G}^{\pm}(\mathbf{P}, \omega) | \mathbf{p}' \rangle \rangle_{\Omega} = \int \frac{d\Omega}{4\pi} \langle \mathbf{p} | \mathcal{G}^{\pm}(\mathbf{P}, \omega) | \mathbf{p}' \rangle , \quad (8)$$

where we average over the angle between \mathbf{P} and \mathbf{p} .

$$\begin{aligned} \langle p | T_{l' l}^{(JST) \pm}(P, \omega) | p' \rangle &= V_{l' l}^{(JST)}(p, p') + \sum_{l''} \int \frac{k^2 dk}{(2\pi)^3} V_{l' l''}^{(JST)}(p, k) \\ &\langle k | \mathcal{G}^{\pm}(P, \omega) | k \rangle \langle k | T_{l'' l}^{(JST) \pm}(P, \omega) | p' \rangle , \end{aligned} \quad (9)$$

In the course of this work we shall discuss two different approximation schemes for the intermediate two-particle propagator in the T-matrix calculation. The formulas for the in medium T-matrix approximation in nuclear matter with partial wave decomposition can be found in Ref. [17].

• Self-consistent solution

The self-consistent solution uses off-shell nucleon propagators in the ladder diagrams (Eq. 4). The imaginary part of the self-energy is defined by the T-matrix in the following way

$$\begin{aligned} \text{Im}\Sigma^+(p, \omega) &= \frac{1}{8\pi} \sum_{(JST)l} (2T+1)(2J+1) \int \frac{d\omega'}{2\pi} \int \frac{d^3 k}{(2\pi)^3} \\ &\langle (\mathbf{p} - \mathbf{k})/2 | \text{Im}T_{ll}^{(JST)} + (|\mathbf{p} + \mathbf{k}|, \omega + \omega') | (\mathbf{p} - \mathbf{k})/2 \rangle \\ &A(k, \omega) \left(f(\omega') + b(\omega + \omega') \right) , \end{aligned} \quad (10)$$

where

$$b(\omega) = \frac{1}{e^{\omega/T} - 1} \quad (11)$$

is the Bose distribution. The real part of the self-energy is the sum

$$\text{Re}\Sigma(p, \omega) = \Sigma_{HF}(p) + \Sigma_d(p, \omega) \quad (12)$$

of the Hartree-Fock term

$$\begin{aligned} \Sigma_{HF}(p) = \frac{1}{8\pi} \sum_{(JST)l} (2T+1)(2J+1) \int \frac{d\omega}{2\pi} \int \frac{d^3k}{(2\pi)^3} \\ V_{ll}^{(JST)}(|\mathbf{p} - \mathbf{k}|/2, |\mathbf{p} - \mathbf{k}|/2) A(k, \omega) f(\omega) , \end{aligned} \quad (13)$$

and the dispersive contribution to real part of the self-energy

$$\Sigma_d(p, \omega) = \mathcal{P} \int \frac{d\omega'}{\pi} \frac{-\text{Im}\Sigma^+(p, \omega')}{\omega - \omega'} . \quad (14)$$

The solution of Eqs. (9), (10), (13), (14), and (3) is obtained by iteration with the constraint

$$4 \int \frac{d\omega}{2\pi} \int \frac{d^3p}{(2\pi)^3} A(p, \omega) f(\omega) = \rho , \quad (15)$$

where ρ is the assumed density of the nuclear matter. Numerical methods used in the solution of the self-consistent T-matrix equations are presented in an appendix.

• Quasi-particle approximation

The quasi-particle solution is obtained by using mean-field propagators in the T-matrix equation.

$$G_{mf}^\pm(p, \omega) = \frac{1}{\omega - \xi_p \pm i\epsilon} , \quad (16)$$

where $\xi_p = \omega_p - \mu$ is the mean-field energy measured with respect to the Fermi energy, and the mean-field quasi-particle energy is of course $\omega_p = p^2/(2m) - \Sigma_{HF}(p)$. More generally, the self-consistent real part of the self-energy (12) can also be used to define the quasi-particle energy. The density is given by

$$\rho = 4 \int \frac{d^3p}{(2\pi)^3} f(\xi_p) . \quad (17)$$

Analogously the expressions for the self-energies in the quasi-particle approximation take the form

$$\begin{aligned} \Sigma_{HF}(p) = \frac{1}{8\pi} \sum_{(JST)l} (2T+1)(2J+1) \int \frac{d^3k}{(2\pi)^3} \\ V_{ll}^{(JST)}(|\mathbf{p} - \mathbf{k}|/2, |\mathbf{p} - \mathbf{k}|/2) f(\xi_k) , \end{aligned} \quad (18)$$

$$\begin{aligned} \text{Im}\Sigma^+(p, \omega) = \frac{1}{8\pi} \sum_{(JST)l} (2T+1)(2J+1) \int \frac{d^3k}{(2\pi)^3} \\ < (\mathbf{p} - \mathbf{k})/2 | \text{Im}T_{ll}^{(JST)} + (|\mathbf{p} + \mathbf{k}|, \omega + \xi_k) | (\mathbf{p} - \mathbf{k})/2 > \\ & \quad \left(f(\xi_k) + b(\xi_k + \omega) \right) . \end{aligned} \quad (19)$$

The dispersive contribution to the real part of the self-energy can be obtained from the dispersion relation (14). Note that there is no need for an iteration procedure in the solution of the T-matrix equation in the quasi-particle approximation, when using Hartree-Fock single particle energies, as in this work. Once the mean-field self-energy is calculated, the T-matrix can be obtained as

$$\begin{aligned} < p | T_{l'l}^{(JST)} \pm (P, \omega) | p' > = V_{l'l}^{(JST)}(p, p') + \sum_{l''} \int \frac{k^2 dk}{(2\pi)^3} V_{l'l''}^{(JST)}(p, k) \\ & \quad \frac{\langle 1 - f(\xi_{p1}) - f(\xi_{p2}) \rangle_\Omega}{\omega - \langle (\xi_{p1} + \xi_{p2}) \rangle_\Omega \pm i\epsilon} < k | T_{l''l}^{(JST)} \pm (P, \omega) | p' > , \\ & \quad \mathbf{p}_{1,2} = \mathbf{P}/2 \pm \mathbf{k} . \end{aligned} \quad (20)$$

For numerical convenience, we calculate the angle average separately in the numerator and in the denominator of the two-particle propagator in the above equation. The spectral function is then calculated using Eq. (19), the dispersion relation (14), and the definition (3). If the spectral function presents a quasi-particle peak around the energy ξ_p , the quasi-particle approximation can be trusted.

Of course an iterative improvement of the single particle energies using the real part of the self-energy obtained in the T-matrix or G-matrix approximation is possible [4, 5]. Such an iterative scheme requires in principle the introduction of BCS-like single particle energies in the presence of pairing. This can be calculated in a quasi-particle version of the formalism used in Sect. 4. However the actual implementation of this approach is quite tedious and we restrict ourselves to the Hartree-Fock single particle energies and to the normal Fermi-liquid phase for the the quasi-particle approximation.

A common property of all the T-matrix approaches to the nuclear matter is the appearance of strong pairing in channels with attractive interactions. As the temperature is lowered a singularity builds up in the T-matrix at zero total momentum and energy. For the quasi-particle scheme it leads to the Thouless criterion for T_c , which is equivalent to weak coupling BCS [9]. The inclusion of self-energy corrections in the normal fermion propagators generalizes this criterion, giving more general equations for the critical temperature. In section 4 we shall derive equations valid also below T_c .

3 Pseudogap formation in finite temperature nuclear matter

Numerical results presented in this, and subsequent sections were obtained using a Yamaguchi separable potential of rank one [18]. The momenta of all the nucleons are restricted to $|p| < 700$ MeV. The coupling strengths of the original Yamaguchi parameterization are slightly adjusted to reproduce the scattering length in vacuum as obtain from the Yamaguchi potential without cutoff in momenta of nucleons

$$V(k, p) = \sum_{\alpha=^1S_0, ^3S_1} \lambda_\alpha g(k)g(p) ,$$

$$g(p) = \frac{1}{p^2 + \beta^2} , \quad (21)$$

with $\lambda_{^1S_0} = -.841$ GeV², $\lambda_{^3S_1} = -.8591$ GeV², and $\beta = 285.9$ MeV. For large momenta the effect of the cutoff is significant. Nevertheless, the following calculation is a helpful illustration, presenting all the basic phenomena related to the superfluidity in nuclear matter, and describing qualitatively the behavior around the Fermi energy. The binding energy of the deuteron and the critical temperature (in the quasi-particle approximation) are changed within few percent by the introduction of the cutoff.

All the results are calculated for nuclear density $\rho = .45\rho_0$. At higher densities, a resonance appears in the two-particle Green's function below the Fermi energy. This happens for temperatures above T_c , according to the Thouless criterion. This statement is strongly dependent on the assumed interaction and the resulting deuteron wave function. This phenomenon is not related to the main subject of this work. We postpone the discussion of this topic, using more realistic parameterizations of the momentum distribution of the deuteron, to another work and restrict ourselves to low density nuclear matter in the following. The Yamaguchi potential has also the practical advantage, that the critical temperature and the energy gap are relatively (somewhat unrealistically) high [8]. The strength of the pairing simplifies the numerics, and is helpful in illustrating qualitatively the physical effects. In Ref. [11] we have studied the self-consistent T-matrix approximation at normal nuclear density and high temperature. However we were not able to perform similar calculations at small temperatures (around and below the critical temperature) with the limited resolution in energy, because the single-particle width becomes very small at the Fermi energy (See appendix).

3.1 Quasi-particle approximation

The spectral function in the quasi-particle approximation has been calculated in several works [5, 8, 19, 20], in the T-matrix or Brueckner schemes. Calculations using the T-matrix approximation for the fermion self-energy show very strong pairing in channels with attractive interactions. At a critical temperature a pole appears in the T-matrix. For the interaction here chosen, it appears first in the in the 3S_1 channel. It signals the formation of neutron-proton bound states (with zero binding energy, since the pole in the T-matrix appears at zero total momentum and at the Fermi energy) [9, 8], for even lower temperature it is preferable

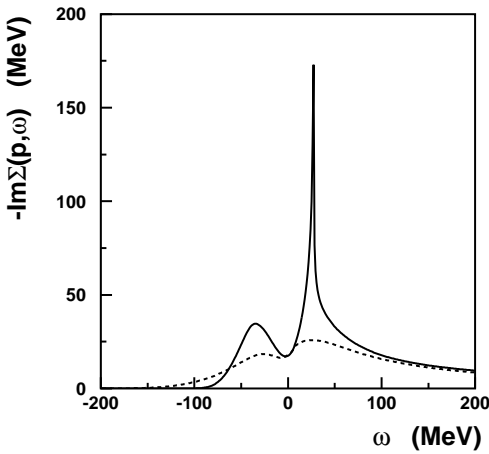


Figure 1: Imaginary part of the self-energy $-\text{Im}\Sigma(p, \omega)$ as function of the energy for $p = 0$ and $p = 175$ MeV (solid and dashed lines respectively), calculated in the quasi-particle approximation for the T-matrix at $\rho = .54\rho_0$, and $T = 5.1$ MeV (slightly above $T_c=5.03$).

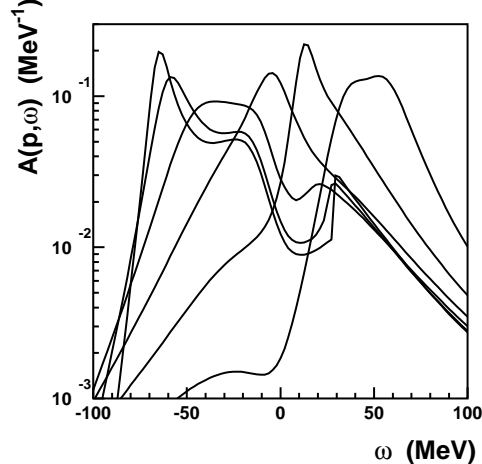


Figure 2: Spectral function $A(p, \omega)$ for several values of momentum as function of energy for the same parameters as in Fig. 1. The lines correspond to $p = 0, 70, 140, 210$ and 350 MeV, according to the position, from left to right, of the largest peak in the spectral function.

for the system to condense into nucleon-nucleon pairs instead of remaining in the Fermi-liquid phase. At temperatures slightly above T_c , the T-matrix is strongly peaked for small values of total momentum and small energy. It is a precursor of the singularity in the T-matrix at the critical temperature. One of the consequences of this singularity is a very unusual form of the imaginary part of the self-energy (Fig. 1). The imaginary part of the self-energy $\text{Im}\Sigma^+(p = 0, \omega)$ has a peak for $\omega = -\xi_{p=0}$. Not surprisingly, the spectral function exhibits also a nontrivial structure, with two or more peaks (Fig. 2). The spectral function is not of a Fermi-liquid type.

The appearance of two peaks in the spectral function above T_c was broadly discussed in high T_c superconductivity under the name of pseudogap formation [21, 22, 23, 24, 25, 26]. The quasi-particle approximation represents only the first iteration in the self-consistent calculation of the nucleon spectral function. Thus, it fails to describe the feedback of the pseudogap on the value of the T-matrix in the vicinity of the Fermi energy. This leads to quantitative difference between the self-consistent and the quasi-particle calculations. The critical temperature is 1.63 MeV for the self-consistent calculation and 5.03 MeV in the quasi-particle approximation. The form of the spectral function is different in the two approximations [11]. The strong differences between the quasi-particle approximation and the self-consistent solution indicate that for strongly interacting systems (having bound or almost bound states in vacuum) the usual approximation of the spectral function by a quasi-particle peak fails already above T_c . Another difference already mentioned in [11] is that the imaginary part of the self-energy has a singularity in the quasi-particle approximation; in the self-consistent calculation this singularity is smeared out. In Fig. 3 we plot the position of the maxima of the peaks in the spectral function as function of the position of the quasi-particle pole ζ_p :

$$\zeta_p - \frac{p^2}{2m} - \text{Re}\Sigma(p, \zeta_p) + \mu = 0 . \quad (22)$$

Clearly two peaks are visible in the spectral function on two sides of the Fermi energy. The dominant peak follows approximately the position of the quasi-particle pole. However, a subdominant peak is found on the other side of the Fermi energy, recalling the effect of an energy gap in the superfluid phase. The effect was named a pseudogap, since the energy gap in the spectral function occurs without pairing condensate and the superfluid density is zero. Close to the Fermi energy the subdominant peak disappears. The position of the quasi-particle peak (solution of Eq. 22) is relatively smooth as a function of momentum, in both the quasi-particle approximation and in the self-consistent solution. There is no sharp variation of the effective mass near the Fermi energy.

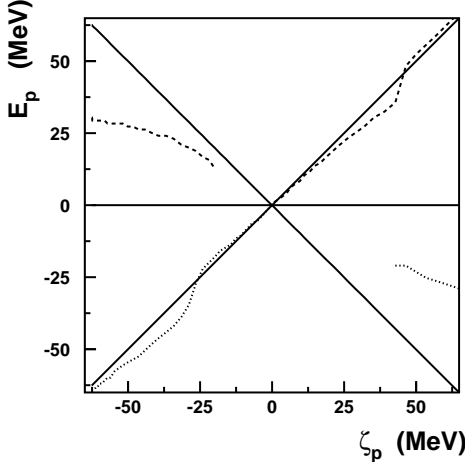


Figure 3: The positions of the largest peaks of the spectral function at positive and negative energies (dotted and dashed lines) as function of the energy of the quasi-particle pole, for the same parameters as in Fig. 1. The solid lines denote the two asymptotic branches in the BCS solution $E_p = \pm \zeta_p$ and the Fermi energy $E_p = 0$.

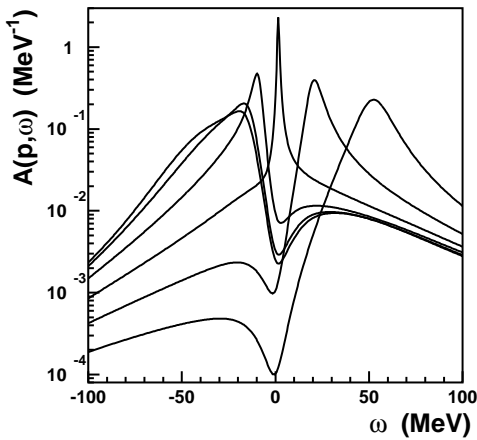


Figure 4: Spectral function for several values of momentum as function of energy. The lines correspond to $p = 0, 70, 140, 210$ and 350 MeV, according to the position, from left to right, of the largest peak in the spectral function. The results were obtained in the self-consistent scheme at $T = 1.7$ MeV (slightly above $T_c = 1.63$ MeV) and $\rho = .45\rho_0$.

3.2 Self-consistent solution

The self-consistent solution has a similar behavior around the critical temperature as the quasi-particle approximation: at the critical temperature the T-matrix has a singularity at zero total momentum and energy, and for temperatures above T_c , the T-matrix is strongly peaked for small values of energy and total momentum. This leads to a pseudogap structure in the spectral function (Fig. 4). This pseudogap structure is again similar to the superfluid gap. Two peaks of the spectral function are located on both sides of the Fermi energy. The dominant peak (with the larger weight) is the one whose energy is the closest to the energy of the quasi-particle pole. Please note that for momenta close to the Fermi momentum there is only one peak in the spectral function (the curve corresponding to $p = 210$ MeV in Fig. 4). In Fig. 5 the dispersion of the two peaks of the spectral function is presented. The dispersion of the maximum of the two peaks is very reminiscent of the superfluid dispersion relations $E_k = \pm \sqrt{\zeta_k^2 + \Delta(k)^2}$, where $\Delta(k)$ is the pseudogap. At the Fermi energy the separation between the two peaks should be equal to twice the value of the pseudogap. However, close to the Fermi energy only one, dominant peak of the spectral function survives. Its width is small close to the Fermi energy, and the position of its maximum is given by the energy of the quasi-particle pole ζ_p .

It is difficult to devise a self-consistent approximate scheme, using a two-pole ansatz for the spectral function. Usually such a procedure would require, when iterating Eq. (10), the introduction of additional poles in the spectral function. A self-consistent approximate solution in the pseudogap region can be obtained only in the pairing approximation [23], i.e. using a mean-field propagator on the right-hand side of Eq. (10). If additional assumptions are made for the T-matrix in the pseudogap region, a self-consistent approximation scheme with superfluid-like ansatz for the spectral function can be obtained [23]. However, the self-consistent solution indicates (Fig. 5), that the pseudogap picture [23] of single-particle excitations above T_c is not entirely correct. Moreover, the energy of the quasi-particle pole is different from the Hartree-Fock energy. The imaginary part of the self-energy and its energy dependence are usually non-negligible.

In Fig. 6 the integrated weights of the two peaks in the spectral function are presented. The weight of the peak is obtained by integrating the spectral function on the same side of the Fermi energy. Although qualitatively the weight of the two parts of the spectral function follows the superfluid result $N_i(k) = \frac{1}{2} \left(1 \pm \frac{\zeta_k}{E_k} \right)$, we could not fit the weight N_i using this law. This is not surprising since the two peaks

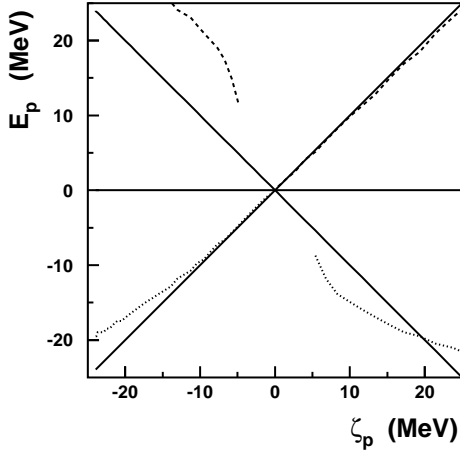


Figure 5: The positions of the two peaks of the spectral function (dotted and dashed lines) as function of the energy of the quasi-particle pole, for the same parameters as in Fig. 4. The solid lines denote the two asymptotic branches in the BCS solution $E_p = \pm \zeta_p$ and the Fermi energy $E_p = 0$.

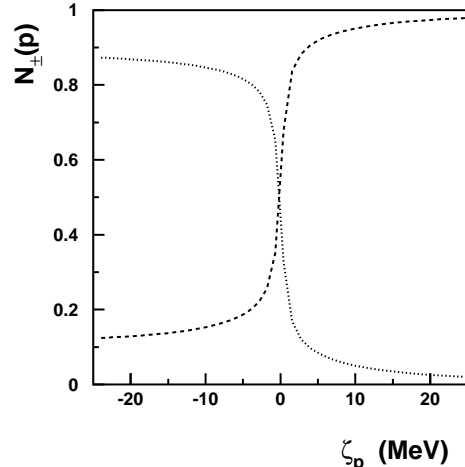


Figure 6: The weight of the peaks of the spectral function at positive and negative energies, for the same parameters as in Fig. 4.

are very broad, and, moreover close to the Fermi energy where the effect of the pseudogap should be the clearest, the two peaks merge into one. The sum of the weights of the two peaks gives of course 1.

The nucleon momentum distribution is presented in Fig. 7. The solid line was obtained using the self-consistently calculated spectral function

$$n(p) = \int \frac{d\omega}{2\pi} A(p, \omega) f(\omega) . \quad (23)$$

The dotted line denotes the result of the quasi-particle approximation for the spectral function

$$n(p) = f(\zeta_p) , \quad (24)$$

where ζ_p denotes the position of the quasi-particle pole, i.e the solution of Eq. (22). Nucleon scattering (nonzero imaginary part of the self-energy in A) leads to a considerable broadening of the momentum distribution. This is another indication that the quasi-particle approximation is not reliable for nuclear matter around the critical temperature.

4 Pairing and the T-matrix approximation

In the superfluid phase the nuclear matter develops a superfluid energy gap and non-zero anomalous fermion propagators. The usual BCS theory is limited to mean-field approximations to the self-energy and to the superfluid gap. Formally T-matrix equations can be written for the normal propagators and anomalous propagators [27, 22]. As before, T-matrix enters in the calculation of the self-energy in place of the interaction potential. But also a generalized T-matrix, between the anomalous propagators enters in the calculation of the anomalous self-energy.

The resulting equations are, however, very difficult and no solution in this scheme has been presented. In the following we will present the simplest generalization of the T-matrix and BCS schemes, allowing for the calculation of the spectral function in the superfluid phase. It is known that there is a link between the T-matrix and the BCS theory at the critical temperature. The critical temperature in the BCS theory is related to the appearance of a singularity in the T-matrix at zero energy [9]. It is a manifestation of more general relation between the T-matrix fermion scattering and pairing, and the BCS gap equation. This

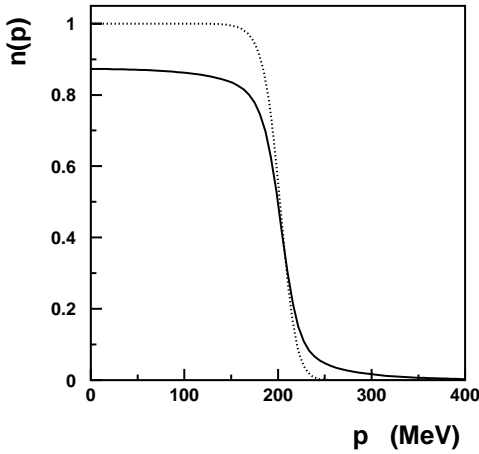


Figure 7: Nucleon momentum distribution obtained from the spectral function (Eq. 23) (solid line) and using the quasi-particle pole approximation for the spectral function (dotted line), for the same parameters as in Fig. 4.

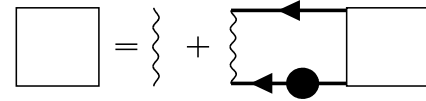


Figure 8: Diagrammatic representation of the T-matrix equation in the superfluid phase. The thick line denotes the off-shell normal fermion propagator, the thick line with a dot denotes the full fermion propagator including the anomalous self-energy, the wavy line denotes the interaction and the box stands for the T-matrix.

relation was observed long time ago by Kadanoff and Martin [10]. They proposed to use one mean-field fermion propagator and one BCS two-pole fermion propagator in the ladder of the T-matrix diagram¹ :

$$\begin{aligned}
 & \langle \mathbf{p} | T_{\alpha' \beta' \alpha \beta}^{\pm}(\mathbf{P}, \omega) | \mathbf{p}' \rangle = V_{\alpha' \beta' \alpha \beta}(\mathbf{p}, \mathbf{p}') \\
 & + \int \frac{d^3 k}{(2\pi)^3} \int \frac{d\omega'}{2\pi} \int \frac{d\omega''}{2\pi} V_{\alpha' \beta' \gamma \delta}(\mathbf{p}, \mathbf{k}) \\
 & \frac{A(\mathbf{P}/2 + \mathbf{k}, \omega' - \omega'') A_s(\mathbf{P}/2 - \mathbf{k}, \omega'') (1 - f(\omega' - \omega'') - f(\omega''))}{\omega - \omega' \pm i\epsilon} \\
 & \langle \mathbf{k} | T_{\gamma \delta \alpha \beta}^{\pm}(\mathbf{P}, \omega) | \mathbf{p}' \rangle ,
 \end{aligned} \tag{25}$$

where A is the spectral function without anomalous self-energy, which we will call in the following normal fermion spectral function, and which takes the form

$$A(\mathbf{p}, \omega) = 2\pi\delta(\omega - \xi_p) , \tag{26}$$

in the quasi-particle approximation, and A_s is the spectral function with anomalous self-energy, which we call full fermion spectral function in the rest of the paper (Fig 8). In the mean-field approximation it takes the usual BCS form

$$A_s(\mathbf{p}, \omega) = 2\pi \left(\frac{E_{\mathbf{k}} + \xi_k}{2E_{\mathbf{k}}} \delta(\omega - E_{\mathbf{k}}) + \frac{E_{\mathbf{k}} - \xi_k}{2E_{\mathbf{k}}} \delta(\omega + E_{\mathbf{k}}) \right) , \tag{27}$$

where

$$E_{\mathbf{k}} = \sqrt{\xi_k^2 + \Delta(\mathbf{k})^2} . \tag{28}$$

Using (25) the gap equation can be written as

$$\sum_{\alpha \beta} \int \frac{d^3 p'}{(2\pi)^3} \langle \mathbf{p} | \text{Re} T_{\alpha' \beta' \alpha \beta}^{\pm -1}(\mathbf{P} = \mathbf{0}, \omega = 0) | \mathbf{p}' \rangle \Delta_{\alpha \beta}(\mathbf{p}') = 0 , \tag{29}$$

¹We use the real time formalism also in the superfluid phase [28], with energies measured with respect to the Fermi energy.

the relation between Δ and $\Delta_{\alpha\beta}$ is given later. The limit of the above equation when $\Delta = 0$ in the T-matrix equation, gives the Thouless criterion for T_c . The meaning of Eq. (29) is, however, more general. It states that the gap equation is equivalent to requiring that the singularity of the T-matrix remains at zero energy and momentum for all temperatures below T_c . The principle of conserving approximation, in the sense of Kadanoff and Baym [14], requires the use of the normal fermion mean field propagator (without anomalous self-energy) on the right hand side of Eqs. (10) and (13).

In the above equations we have assumed that the ground state is time-reversal invariant. Thus, the full fermion propagator G_s is still diagonal in spin-isospin indices [29, 30]. However, the full spectral function and the full propagator depend in general on the direction of the momentum. Also the T-matrix would then depend on the direction of the total momentum of the pair.

In principle the pairing approximation of Kadanoff and Martin can be used to calculate the spectral properties of the nuclear matter in the superfluid phase using the quasi-particle approximation. However, as we have seen, the quasiparticle approximation becomes unreliable in the case of strong attractive interaction between fermions, with bound or almost bound states in vacuum. As discussed in models of high T_c superconductivity, the crossover region between the BCS pairing and the boson condensation, cannot be described using mean-field fermion propagators for the calculation of the T-matrix. The same is true in nuclear matter for with the Yamaguchi interaction in the T-matrix approximation, because of the pseudogap formation in the spectral function (Sec. 3). At higher densities, in particular at the saturation density, the pairing gap is expected to be smaller and the BCS theory is correct. Certainly calculations using more realistic interactions for several densities, including the modification of single-particle energies and finite quasi-particle width, would clarify at which densities, if any, the crossover-like behavior between the BCS pairing and the boson condensation occurs. One way to generalize the Kadanoff-Martin approach was proposed by the Chicago group [23, 24]. From the observation that a pseudogap in the spectral function forms above T_c , the authors of Refs. [23, 24] proposed to use one mean-field and one full propagator in the T-matrix equation. The full propagator would include self-consistently the normal self-energy in the T-matrix approximation (defined by (18) and (19)), and, below T_c , also the anomalous self-energy (defined by the superfluid gap (29)). In actual calculations, the authors of [23, 24] used an approximate BCS-like form also the normal self-energy in the vicinity and below T_c . The spectral function is then given in an analytical form by the superfluid gap and by a pseudogap, defined by the singularity of the T-matrix for small energy and small total momentum. This approach represents an improvement over the quasi-particle approximation, because it takes into account the pseudogap formation in the calculation of the T-matrix. Also its a very nice illustration of the mechanism of the pseudogap formation and of the two-fermion excitations close to the Fermi energy [23]. The pseudogap, as well as the superfluid gap, causes the formation of an energy gap in the two-fermion excitations around the Fermi energy, very similar to the one postulated in [4]. However, the self-consistent spectral function calculated in Sec. 3.2 shows only partly a pseudogap. The position of the subdominant peak in the spectral function does not follow the relation expected from a pseudogap energy dispersion relation. Also close to the Fermi energy only one peak in the spectral function is present. One could use the full spectral function instead of the pseudogap approximation for one of the propagators in the T-matrix equation. Thus, the correct dispersion of the peaks in the spectral function would be taken into account self-consistently. However, it turns out that the numerical cost of a calculation in the pairing approximation with one off-shell propagator and of a full self-consistent calculation is similar. Also the use of the mean-field propagator in the calculation of the self-energy (19), as required in the pairing approximation, leads to a singularity in the self-energy at T_c . No such effect is present in the self-energy from the self-consistent calculation [11].

Therefore, we shall seek a generalization of the self-consistent T-matrix equations in the superfluid phase, including the off-shell fermion propagators in the T-matrix equation and in the self-energy calculation. Since the T-matrix equation in the pairing approximation is related to weak-coupling BCS equation [10], we will use a mean-field approximation for the anomalous self-energy. Indeed the superfluid gap equation (Fig 9)

$$\Delta_{\alpha\beta}(\mathbf{p}) = - \sum_{\alpha'\beta'} \int \frac{d\omega}{2\pi} \int \frac{d^3k}{(2\pi)^3} V_{\alpha\beta\alpha'\beta'}((\mathbf{p} - \mathbf{k})/2, (\mathbf{p} - \mathbf{k})/2) B_{\alpha'\beta'}(\mathbf{k}, \omega) f(\omega) , \quad (30)$$

can be related to the T-matrix equation, using strong coupling BCS equations, with frequency independent gap parameter [31, 32] (Fig 10)

$$G_s^+(\mathbf{p}, \omega) = G^+(\mathbf{p}, \omega) - \frac{1}{4} \sum_{\alpha\beta} \Delta^{\alpha\beta}(\mathbf{p}) F_{\alpha\beta}^{\dagger+}(\mathbf{p}, \omega) \quad (31)$$

$$F_{\alpha\beta}^{\dagger+}(\mathbf{p}, \omega) = G^-(-\mathbf{p}, -\omega) G_s^+(\mathbf{p}, \omega) \Delta_{\alpha\beta}^\dagger(\mathbf{p}) , \quad (32)$$

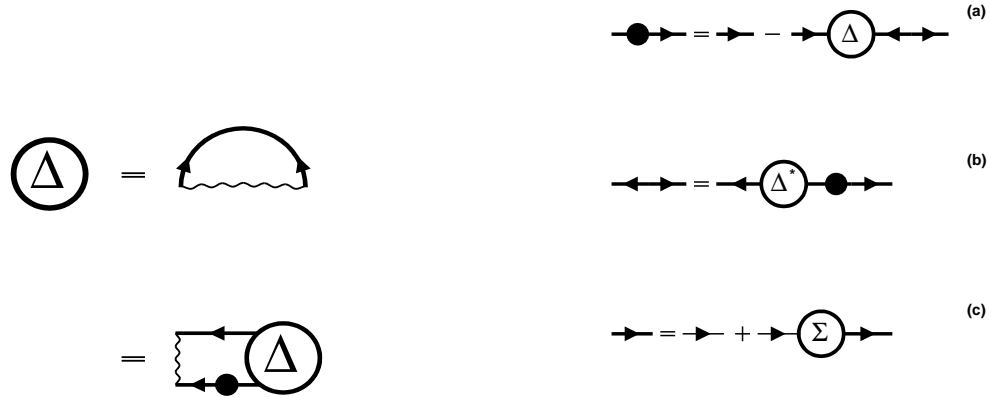


Figure 9: Diagrammatic representation of the gap equation (30) (first line). The thick line with two arrows denotes the anomalous propagator and the circle with the letter Δ denotes the pairing gap, other symbols as in Fig. 8. The equality in the second line, is equivalent to Eqs. (29), (34).

Figure 10: Diagrammatic representation of the BCS Dyson equation. (a) represents the resummation of the anomalous self-energy in the nucleon propagator in the superfluid phase (Eq. 31), (b) represents the equation for the anomalous propagator (Eq. 32) and (c) represents the usual resummation of the self-energy (the circle with the letter Σ). Symbols as in Figs. 8, 9.

where G_s is the full fermion Green's function, including the anomalous self-energy (G is reserved, from now on, to the normal Green's function including only the normal self-energy). The anomalous propagator spectral function is

$$B_{\alpha\beta}(\mathbf{p}, \omega) = -2\text{Im}F_{\alpha\beta}^+(\mathbf{p}, \omega) . \quad (33)$$

Using (32) in the gap equation (30), and using the spectral representation of the propagators G and G_s one obtains

$$\frac{\Delta_{\alpha'\beta'}(\mathbf{p}) + \int \frac{d^3k}{(2\pi)^3} \int \frac{d\omega}{2\pi} \int \frac{d\omega'}{2\pi} V_{\alpha'\beta'\gamma\delta}(\mathbf{p}, \mathbf{k})}{\omega} \frac{A(\mathbf{P}/2 + \mathbf{k}, \omega - \omega') A_s(\mathbf{P}/2 - \mathbf{k}, \omega) (1 - f(\omega - \omega') - f(\omega'))}{\omega} \Delta_{\gamma\delta}(\mathbf{k}) = 0 . \quad (34)$$

Thus, the gap equation for the superfluid gap is equivalent to the condition that Δ is the zero eigenvalue vector of the real part of the inverse T-matrix (Eq. 29), i.e. Eqs. (29), (34) and (30) are equivalent. However, here the T-matrix is given by the expression (25), with the spectral functions A and A_s being obtained from the solution of (31) ($A(p, \omega) = -2\text{Im}G^+(p, \omega)$, $A_s(\mathbf{p}, \omega) = -2\text{Im}G_s^+(\mathbf{p}, \omega)$).

The set of equations (25), (31), and (30), defines a consistent approximation scheme for the nucleon self-energy below T_c . In this approach the singularity of the T-matrix is always at zero energy and zero total momentum, the same is true in the BCS approach [10]. However here we include the contribution of the scattering and resonant pairs to the self-energy, through Eq. (10), as well as of the condensed pairs, through the anomalous self-energy. In the region of intermediate coupling strength, between the weak BCS and the Bose condensation, the contribution of the T-matrix to the normal self-energy is important [27, 21, 23, 24], and leads to a pseudogap formation.

There is one more technical obstacle before using this scheme in actual calculations. In the superfluid phase the full propagator $G_s(\mathbf{p}, \omega)$ depends on the direction of the momentum \mathbf{p} , and the T-matrix depends on the direction of the total momentum. This dependence introduces tremendous difficulties in the numerical solution of the T-matrix (25) and the BCS Dyson equation (31). Also in the T-matrix calculation we have used partial-wave expansion, enabled by the angle averaging of the two-fermion propagator in

the ladder diagrams. On the other hand, the solution of the superfluid gap equation, which is equivalent to the calculation T-matrix equation at zero total momentum, requires no angular averaging of the two propagators in (32). In the BCS theory an approximate decoupling of different angular momentum gaps is obtained [33]. In that case the gap equation in each partial wave approximately decouple, i.e. we can use a different propagator G_s in each of the partial wave gap equations. In nuclear physics the situation is more complicated due to the coupled partial waves in the T-matrix. If we include the coupled partial waves, we cannot use the partial wave decoupling of the gap equations (e.g. $^3S_1 - ^3D_1$). Also in the nuclear matter we can in general have two superfluid gaps for the same partial wave but with different total angular momentum and isospin (e.g. 1S_0 and 3S_1). Moreover, we want to use the angular averaged two-nucleon propagator in the T-matrix equation. Thus, the corresponding gap equations in different channels will be coupled through the dependence of the full fermion propagator G_s on the anomalous self-energy. In practice only the gap corresponding to one channel would be non-zero, the one with the strongest pairing at a given temperature and density. The T-matrix in other channels would have the singularity pushed away from the Fermi energy due to the energy gap originating from the paired channel. Of course this does not exclude phase transitions between pairing in different channels, when changing the temperature or density.

In order to simplify the description of the full fermion propagator we shall use an angle averaged anomalous self-energy in (31). This approximation simplifies also the gap equation [30], in particular the superfluid gap for non-zero angular momentum can be taken as real and independent of the projection of the angular momentum [34]. Of course such an assumption for the superfluid gap is only an approximation, and in some cases the true ground state of the nuclear matter may be described by more complicated angle dependent anomalous propagators. The example of the liquid Helium teaches us that the structure of the anisotropic superfluid order parameter can be very rich [35]. In particular the real order parameter would not lead to the state of lowest energy. However, it is sufficient for consistent and stable T-matrix calculation of the nuclear matter. It would be extremely difficult to implement the most general angle dependent superfluid gap and full fermion propagator in the T-matrix calculation.

As a result the self-consistent T-matrix can be decomposed in partial waves

$$\begin{aligned}
& \langle p | T_{ll'}^{(JST)} \pm (P, \omega) | p' \rangle = V_{ll'}^{(JST)}(p, p') \\
& + \sum_{l''} \int \frac{d^3 k}{(2\pi)^3} \int \frac{d\omega'}{2\pi} \int \frac{d\omega''}{2\pi} V_{ll''}^{(JST)}(p, k) \\
& \langle \frac{A(|\mathbf{P}/2 + \mathbf{p}|, \omega' - \omega'') A_s(|\mathbf{P}/2 - \mathbf{p}|, \omega'') (1 - f(\omega' - \omega'') - f(\omega''))}{\omega - \omega' \pm i\epsilon} \rangle_{\Omega} \\
& \langle k | T_{l'l'}^{(JST)} \pm (P, \omega) | p' \rangle . \tag{35}
\end{aligned}$$

The full fermion Green's function can be written as

$$G_s^+(p, \omega) = \frac{1}{G^+(p, \omega)^{-1} + \Delta^2(p) G^-(p, -\omega)} , \tag{36}$$

where the normal fermion propagator is given by the standard expression and $\Delta(p)$ is the angle averaged total energy gap. The self-energy Σ is given by Eqs. (13) and (10), with the normal spectral function A on the right hand side. The set of gap equations in (JST) channels takes the form

$$\begin{aligned}
& \Delta_l^{(JST)}(p) = - \sum_{l'} \int \frac{d\omega}{2\pi} \int \frac{d\omega'}{2\pi} \int \frac{k^2 dk}{(2\pi)^3} V_{ll'}^{(JST)}(p, k) \\
& \frac{A(k, \omega - \omega') A_s(k, \omega') (1 - f(\omega - \omega') - f(\omega'))}{\omega} \Delta_{l'}^{(JST)}(k) . \tag{37}
\end{aligned}$$

The existence of a non-zero solution of the above equation in a particular channel is equivalent to the presence of a singularity in the T-matrix in that channel at zero total momentum and zero energy. The total, angle averaged energy gap is given by an incoherent sum of contributions in different channels

$$\begin{aligned}
\Delta^2(p) &= \frac{1}{8\pi} \sum_{(JST)l} (2T+1)(2J+1) \Delta_l^{(JST)}(p)^2 \\
&= \frac{1}{8\pi} (2T+1)(2J+1) \sum_l \Delta_l^{(JST)s}(p)^2 , \tag{38}
\end{aligned}$$

where in the last equality we have used the fact that only one channel $(JST)_s$ gives nonzero gap. It is the channel which gives the larger value of $\Delta(p)$. One can notice that using mean-field spectral function in (37), one recovers the BCS gap equations in (JST) channels from [30]. The final equation of the calculation scheme is the expression for the nuclear density

$$\rho = 4 \int \frac{d\omega}{2\pi} \int \frac{d^3 p}{(2\pi)^3} A_s(p, \omega) f(\omega) . \quad (39)$$

It is instructive to write explicitly the full fermion spectral function in terms of the energy gap and the self-energy

$$\begin{aligned} A_s(p, \omega) = & -2 \left(\left(\omega + \xi_p + \text{Re}\Sigma^+(p, -\omega) \right)^2 \text{Im}\Sigma^+(p, \omega) \right. \\ & + \text{Im}\Sigma^+(p, -\omega) \Delta^2(p) + \left(\text{Im}\Sigma^+(p, -\omega) \right)^2 \text{Im}\Sigma(p, \omega) \Big) / \\ & \left(\left((\omega - \xi_p - \text{Re}\Sigma^+(p, \omega)) (\omega + \xi_p + \text{Re}\Sigma^+(p, -\omega)) \right. \right. \\ & - \text{Im}\Sigma^+(p, \omega) \text{Im}\Sigma^+(p, -\omega) - \Delta^2(p) \Big)^2 \\ & \left. \left. + \left(\text{Im}\Sigma^+(p, \omega) (\omega + \xi_p + \text{Re}\Sigma^+(p, -\omega)) \right. \right. \right. \\ & \left. \left. \left. + \text{Im}\Sigma^+(p, -\omega) (\omega - \xi_p - \text{Re}\Sigma^+(p, \omega)) \right)^2 \right) . \end{aligned} \quad (40)$$

It is clear that in order to find the spectral function for energy ω , one has to know the self energy for energy ω and $-\omega$. Therefore, the numerical solution must be performed in a symmetrical interval around the Fermi energy ($\omega = 0$).

5 Nuclear matter in the superfluid phase

We solve numerically the set of equation (35), (10), (40), (37), with the constraint (39) for the same interaction as used in Sec. 3. Eqs. (39) and (37) are solved simultaneously for the superfluid gap $\Delta(k)$ and for the chemical potential μ . Below T_c the gap equation has a nontrivial solution, corresponding to the superfluid phase. For the case of the Yamaguchi interaction, the pairing occurs always in the 3S_1 channel. The T-matrix has a singularity at zero momentum and zero energy in this channel, for all temperatures below T_c . The T-matrix in the 1S_0 channel has no singularity but is strongly peaked near the Fermi energy. For more realistic interaction we expect also pairing in the 1S_0 channel and pairing with higher angular momentum at larger densities. The calculation gives two spectral functions, the normal spectral function $A(p, \omega)$, without the anomalous self-energy, and the full spectral function $A_s(p, \omega)$, obtained from the BCS Dyson equation (31). We have observed that due to strong attractive interaction, and due to the appearance of the singularity in the T-matrix, a BCS-like two peak structure appears in the spectral function A in the pseudogap region. The same is true below T_c (Figs. 12 and 14). The spectral function without anomalous self-energy is very similar as above T_c (Fig. 4). Indeed the imaginary part of the self-energy (Fig. 11) is almost indistinguishable for the two temperatures, except near the Fermi energy². In the full spectral function another mechanism is also responsible for the double peak structure. For all momenta the full spectral function A_s has two peaks situated on both sides of the Fermi energy. Close to the Fermi energy, the superfluid gap in the spectral function is clearly visible (Fig 13). Far from the Fermi energy the modifications of the dominant peak are negligible. The subdominant peak of the spectral function is only slightly modified by the anomalous self-energy. This is what is expected form the usual BCS theory, since the weight of the subdominant superfluid peak in the spectral function $\frac{1}{2} \left(1 - \frac{|\xi_k|}{E_k} \right)$ is becoming small far from the Fermi energy.

The dispersion of the maximum of the peaks of the spectral functions A and A_s illustrates the formation of the superfluid gap (Fig. 15). On the abscissa we plot the energy of the quasi-particle pole in the normal

²As expected the scattering width at the Fermi energy decreases with the temperature.

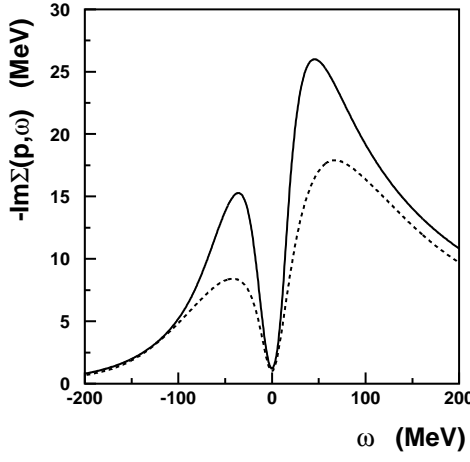


Figure 11: The imaginary part of the self-energy, calculated in the self-consistent T-matrix approximation as function of the energy, for the same parameters as in Fig. 4. The solid and dashed lines denote the results at $p = 0$ and $p = 175$ MeV respectively.

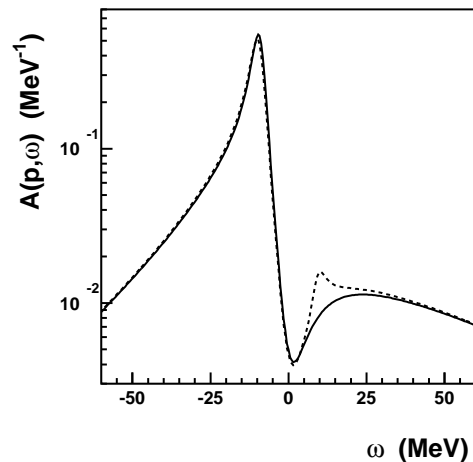


Figure 12: The spectral function $A(p, \omega)$ (solid line) and the spectral function with anomalous self-energy $A_s(p, \omega)$ (dashed line) as function of energy at $p = 140$ MeV. The results were obtained at $T = 1.4$ MeV, and $\rho = .45\rho_0$, corresponding to a superfluid gap of $\Delta(0) = 5.1$ MeV.

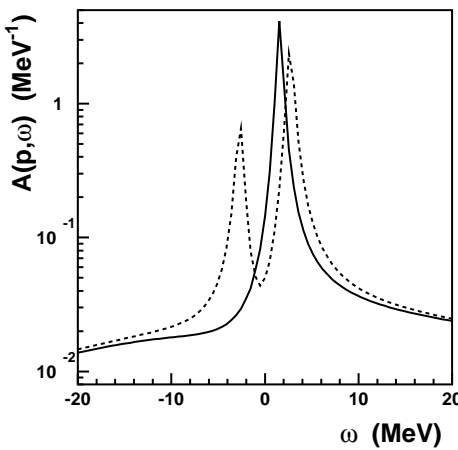


Figure 13: Same as in Fig. 12 but for $p = 210$ MeV.

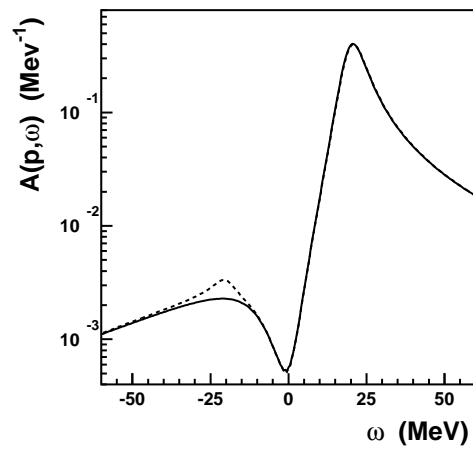


Figure 14: Same as in Fig. 12 but for $p = 280$ MeV.

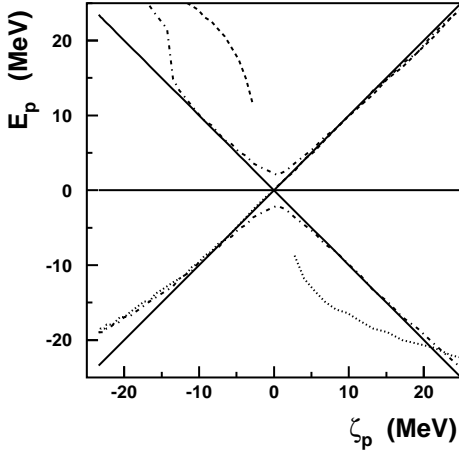


Figure 15: The positions of the two peaks of the normal spectral function (dotted and dotted lines) and of the full spectral function (dash-dotted lines) as function of the energy of the quasi-particle pole, for the same parameters as in Fig. 12. The solid lines represent the two asymptotic branches in the BCS solution $E_p = \pm \zeta_p$ and the Fermi energy $E_p = 0$.

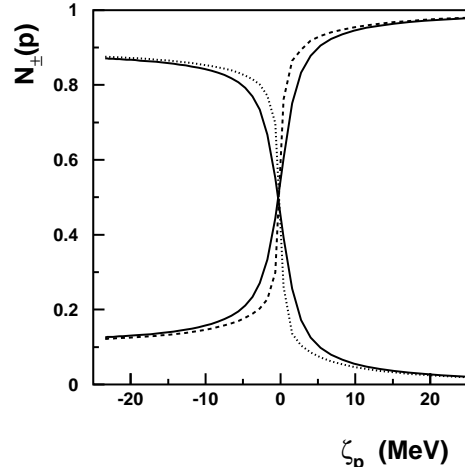


Figure 16: The weight of the peaks of the normal spectral function at positive and negative energies (dashed and dotted lines) and of the peaks of the spectral function with anomalous self-energy (solid lines), for the same parameters as in Fig. 12.

fermion Green's function G . This energy coincides approximately with the maximum of the dominant peak in the spectral function A . This is especially well fulfilled in the vicinity of the Fermi energy. The subdominant peak in the spectral function A is visible for energies further away from the Fermi energy, also its energy does not follow the branch $E_p = -\zeta_p$. Like for the case above T_c , the pseudogap in the spectral function is only qualitatively similar to a superfluid gap. Close to the Fermi energy, the spectral function A is similar as in the normal Fermi liquid. On the other hand, the positions of the peaks of the full spectral function A_s follow the dispersion relation expected for a superfluid matter, especially close to the Fermi energy. An energy gap is clearly visible for $\zeta_p \simeq 0$. Away from the Fermi energy, the positions of the two peaks approach $E_p = \zeta_p$ for the dominant peak and $E_p = -\zeta_p$ for the subdominant peak in the full fermion spectral function. For $|\zeta_p| > 10$ MeV, the positions of the peaks do not follow the BCS energy branches any more. However, one can observe that the dominant peaks in the normal fermion spectral function and in the full fermion spectral function are very close away from the Fermi energy, as expected.

In Fig. 16 are presented the weights of the peaks in the spectral functions A and A_s as function of the energy of the quasi-particle pole of the spectral function A . The peaks in the two spectral functions have qualitatively similar behavior. However, the weight of the dominant (subdominant) peak is smaller (larger) in the full spectral function, than in the normal spectral function. It means that part of the weight of the spectral function is shifted from the dominant to the subdominant peak, as expected from the presence of an additional mechanism of peak doubling in the superfluid phase.

The fermion momentum distribution is plotted in Fig. 17. The finite imaginary part of the spectral function modifies strongly the momentum distribution. The momentum distributions obtained from the spectral functions A and A_s are much broader than the one obtained taking the quasi-particle pole approximation for the spectral function. As expected, the nucleon scattering produces a high momentum tail in the distributions. The effect of the superfluid gap can be seen in the difference between the solid and dashed lines in Fig. 17. As expected [31, 32] the full spectral function A_s gives broader momentum distributions. The BCS broadening with small energy gap results in the smearing of the momentum distribution in an interval $2\Delta(p_F)$ around the Fermi energy. The density given by the quasi-particle approximation to the spectral function A is ~ 1.01 times the actual fermion density given by (39). The densities calculated from the spectral function A and A_s are almost the same.

In Fig. 18 we plot the temperature dependence of the superfluid gap $\Delta(0)$ as function of the temperature.

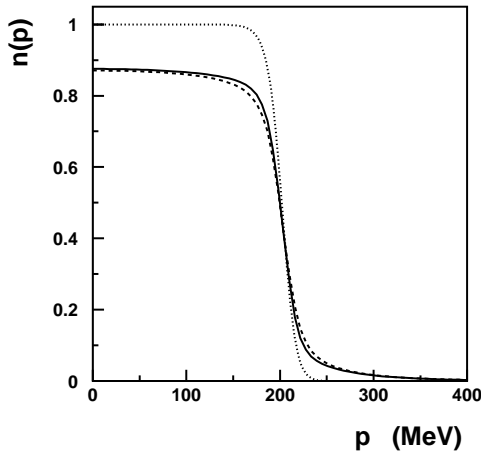


Figure 17: Nucleon momentum distribution obtained from the normal spectral function (solid line), from the full spectral function (dashed line), and using the quasi-particle pole approximation for the spectral function (dotted line), for the same parameters as in Fig. 12.

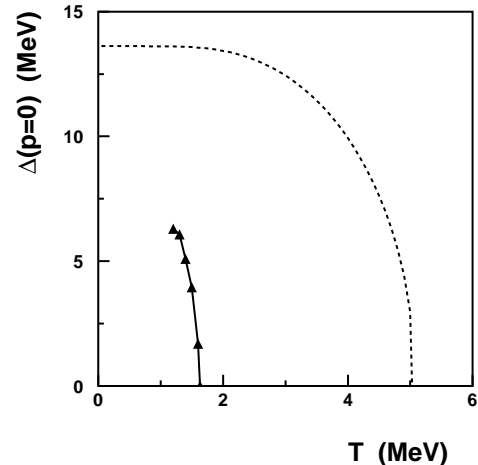


Figure 18: The superfluid energy gap as function of temperature for the BCS theory (dashed line) and for the self-consistent calculation (triangles), for $\rho = .45\rho_0$.

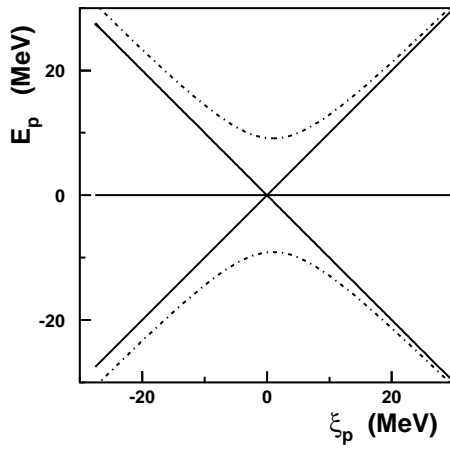


Figure 19: BCS quasiparticles energies as function of the Hartree-Fock single-particle energy, for $T = 1.4$ MeV and $\rho = .45\rho_0$.

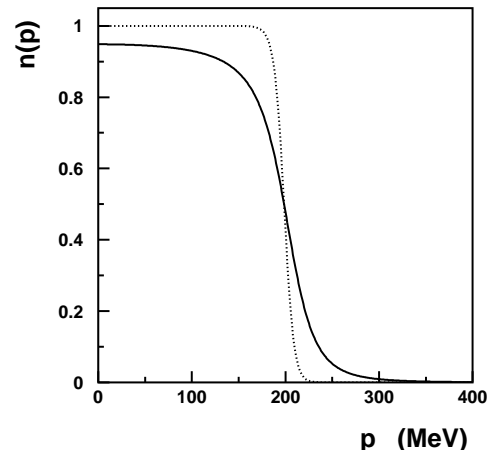


Figure 20: Nucleon momentum distribution for the Hartree-Fock single-particles energies (dotted line) and the BCS nucleon distribution (solid line), for the same parameters as in Fig. 19.

Below $T_c = 1.63$ MeV the superfluid gap rapidly sets in. We could not perform calculations below $T = 1.2$ MeV, due to limited numerical resolution in energy. However, a saturation in the dependence of the superfluid gap can already be observed at the lowest temperatures studied. The dashed line denotes the result of the BCS theory. The critical temperature for the BCS theory is the same as in the quasi-particle approximation, $T_c = 5.03$ MeV. The scattering of nucleons and the pseudogap formation above T_c make the pairing more difficult. In the pairing approximation [24] part of the actual energy gap is due to the pseudogap and part to the superfluid gap. Thus the superfluid transition occurs only when the pseudogap alone is not enough to exclude the pairing. It occurs at a much lower temperature. Another effect may be related to quantitative differences between the quasi-particle and the self-consistent calculations. The real part of the self-energy and the T-matrices are different in the two cases. Below T_c the self-consistent energy gap is always significantly smaller than the BCS result. This is different from the pseudogap pairing approximation [24], where at zero temperature the pseudogap goes to zero and the usual BCS result is recovered. We could not perform calculations at low temperatures, due to limitations in computational resources. However, already in Fig. 18, a saturation of the energy gap in the self-consistent calculation is visible, around $\Delta(0) = 7$ MeV.

For comparison we plot also the dispersion relation for the peaks in the BCS spectral function at $T = 1.4$ MeV: $E_p = \pm \sqrt{\xi_p^2 + \Delta^2(p)}$. Since the energy gap is larger than in the self-consistent calculation the splitting of the two energies in the spectral function is much more pronounced. It should be noted that the condition of weak BCS, $\Delta(0) \ll \xi_{p=0}$, is not really fulfilled in the above case. It is another indication that weak coupling BCS theory with free nucleon-nucleon interaction should not be used in the nuclear matter. The strong modification of the spectral function by the anomalous self-energy in the BCS case is visible also in the fermion momentum distribution (Fig. 20). The BCS fermion distribution is much broader than the Hartree-Fock distribution. Also the density, which is taken to be $\rho = .45\rho_0$ for the BCS fermion distribution is $.43\rho_0$ for the Hartree-Fock distribution.

6 Conclusions

We have presented a new way of performing nuclear matter calculations in the presence of nuclear superfluidity. The starting point is the T-matrix approximation for the nucleon self-energy. It allows to calculate the spectral properties of nucleons in an interacting system, treating on equal footing particle-particle and hole-hole diagrams. It leads also to the formation of Cooper pairs below some critical temperature. Strong scattering in the vicinity of the critical point, leads to a breakdown of the quasi-particle picture, confirming the observation of [11]. This requires the use of self-consistent, and not quasi-particle, fermion Green's functions for the calculation of the self-energy. A more important generalization of the formalism is required to address the superfluid transition. In section 4 such a scheme is presented at least for the case, where the T-matrix approach indicates a second order transition. It consists in the use of off-shell propagators in the T-matrix ladder, one of them including also the anomalous self-energy. In such a way the superfluid gap equation is equivalent to the condition that the T-matrix has a singularity at Fermi energy and zero total momentum for all temperatures below T_c . The full nucleon spectral function includes the anomalous self-energy from the condensed pairs, and the normal self-energy due to nucleon-nucleon scattering. Both contributions are important for strongly attractive potentials in nuclear matter leading to an interplay of the pseudogap and superfluid gap around T_c . The method presented in this work has several important properties

- Above T_c , it leads to a self-consistent T-matrix resummation, which allows for the description of the feedback of the pseudogap formation and of the scattering on the T-matrix.
- It provides a link between the gap equation and the T-matrix equation, at the critical temperature and below.
- It gives the BCS theory in the limit of small scattering rates, unlike the approach [27, 22].
- The value of the energy gap and the critical temperature are strongly reduced, in comparison to the BCS (quasi-particle) results.

When used with realistic nuclear forces, this approach presents a procedure for calculating the nuclear matter properties, taking into account self-consistently single-particle spectral properties and fermion pairing. Both these important questions were not studied up to now in actual nuclear matter calculations. The first

of these problems was discussed in a number of works related to high T_c superconductivity [23, 21, 25]; the first such calculation being presented by Hausmann [26]³. The second question was addressed, to the author's knowledge, only by two groups in condensed matter physics [22, 24]. The work [22] uses a T-matrix resummation with both fermion propagators in the ladder including the anomalous self-energy. However, due to the truncation of the resummation in the anomalous sector, the usual BCS gap equation is used. In that way, the gap equation is not consistent with the T-matrix resummation of the normal self-energy. The approach [4] is similar, i.e. it uses two full propagators in the ladder diagrams. Thus, the gap equation is recovered only for small gap, or is used in its linear form. The work [24] uses the pairing approximation, with one mean-field propagator and one with normal and anomalous self-energies. Both self-energies have a BCS like form. Our approach is a generalization of this procedure, using two off-shell propagators in the T-matrix it allows us to use the off-shell propagator for the calculation of the Hartree-Fock and scattering self-energies (13) and (10), it is not restricted to a BCS like form of the normal self-energy, and it gives the most general T-matrix self-energy scheme above T_c . It should be stressed that there is no reason to neglect off-shellness in one of the propagators in the T-matrix ladder. The consistency with the gap equation requires only to neglect the anomalous self-energy in one of these propagators. The value of the pseudogap goes to zero at low temperature in the pairing approximation [24]. On the other, hand the energy gap in the self-consistent calculation is much smaller than the BCS gap also at low temperatures (Fig. 18).

The numerical results are given for a very simple interaction. We plan to study the superfluid nuclear matter using more realistic separable interactions and also at zero temperature. This would allow to study questions like the effect of pairing⁴ interaction on the ground state energy, the interplay between pairing in isospin 0 and 1 channels, and the pairing in neutron matter. Some more fundamental questions remain also open. We use for the energy gap a mean-field approximation. Moreover, the interaction potential in the gap equation is the free one. Obviously modification of the pairing potential in medium, due to screening, are expected. For consistency the same screened potential should be used in the T-matrix equation for normal nucleon self-energy, meaning significant complications [36]. Another, question is related to the cause of the reduction of T_c . In our calculation both the pseudogap and the nucleon scattering effects are included. To disentangle them the self-consistent calculation should be compared to results of the quasi-particle approximation and of the pairing approximation below T_c .

This work was partly supported by the National Science Foundation under Grant PHY-9605207.

Appendix

In this appendix we sketch the numerical method used in the iterative solution of the coupled equations for the T-matrix, the the self-energy and the spectral function. Special methods must be used for an efficient estimation of multidimensional integrals, over energies and momenta, involved in the calculation of the T-matrix and the self-energy when using off-shell propagators.

Let us enumerate below the steps of the iterative procedure, explaining in details the calculation of the energy integrals. We present the case of a separable potential of rank 1, as used in the actual calculations in this work. In that case the T-matrix in a given channel c is given by

$$\langle k|T^c + (P, \omega)|k' \rangle = \frac{\lambda_c g_c(k) g_c(k')}{1 - \lambda_c J_c(P, \omega)}, \quad (41)$$

where the function J_c depending only on the total momentum and energy is given by

$$\begin{aligned} J_c(P, \omega) = & \int \frac{k^2 dk}{(2\pi)^2} \int d\cos(\Theta) \int \frac{d\omega'}{2\pi} \int \frac{d\omega''}{2\pi} g^2(k) \\ & \frac{A(p_1, \omega' - \omega'') A_s(p_2, \omega'') (1 - f(\omega' - \omega'') - f(\omega''))}{\omega - \omega'' + i\epsilon}, \\ & p_{1,2} = P^2/4 + k^2 \pm P k \cos(\Theta). \end{aligned} \quad (42)$$

³Only Ref. [25] uses real time formalism for numerical calculations of the self-consistent T-matrix, like the present work.

⁴The effect of the off-shellness of the propagators on the ground state energy has not been studied either.

For rank one separable interaction, a nonzero solution of the gap equation (29) is equivalent to the condition $1 - \lambda_c J_c(P = 0, \omega = 0) = 0$ and the momentum dependence of the pairing gap is $\Delta(k) = \Delta(0)g_c(k)/g_c(0)$. Let us present in the following, step by step, one iteration starting from the calculation of the spectral function :

1. Let us assume that the imaginary part of the self-energy is known⁵. The dispersive contribution to the real part of the self-energy can be obtained from (14). The calculation of the spectral functions A and A_s requires also the knowledge of the chemical potential μ and the pairing gap Δ . The condition for superfluidity is checked and if necessary the gap equation (29) is solved, using a numerical procedure for the solution of a nonlinear equation⁶. For each trial value of Δ the chemical potential and the corresponding Hartree-Fock energy are obtained with the constraint (39) and using Eqs. (40) and (13). For each trial value of μ the coupled equations (13), (40), (3), (39) are solved by iteration. As a result we obtain the spectral functions A and A_s .
2. In this step we calculate the T-matrix $T_c(P, \omega)$ for a range of values of total momentum and energy. Let us first calculate the imaginary part of the function $J_c(\omega, P)$

$$\text{Im}J_c(P, \omega) = - \int \frac{d\omega'}{2\pi} \int \frac{k^2 dk}{8\pi^2} \int d\cos(\Theta) A_s(p_2, \omega') (1 - f(\omega')) A(p_1, \omega - \omega') (1 - f(\omega - \omega')) g_c^2(k) + \dots \quad (43)$$

the dots represent a similar term with factors f instead of $(1 - f)$. The above ω' integral is a convolution integral and can be performed using fast Fourier transform algorithms for numerical convolutions. First the two factors in the energy integral are Fourier transformed

$$F_{(s)}(p, t) = \text{FFT} [A_{(s)}(p, \omega)] . \quad (44)$$

Then the function

$$\bar{J}_c(P, t) = - \int \frac{k^2 dk}{8\pi^2} \int d\cos(\Theta) F(p_1, t) F_s(p_2, t) g_c^2(k) , \quad (45)$$

is calculated using standard integration procedures for the two-dimensional momentum integration. The first term in Eq. (43) is obtained by inverse Fourier transform of \bar{J} . Analogously the second term in (43) can be calculated. The real part of J is calculated using a dispersion relation

$$\text{Re}J_c(P, \omega) = \mathcal{P} \int \frac{d\omega'}{\pi} \frac{-\text{Im}J_c(P, \omega)}{\omega - \omega'} . \quad (46)$$

3. The imaginary part of the self-energy (10) can also be written as a sum of two convolution integrals in energy and can be calculated in a similar way as $\text{Im}J$ in the previous point. This gives a next iteration of the single-particle width and the iteration returns to the first point.

A generalization to a separable potential of higher rank is obvious. Since the Fourier transforms are performed before the loop over the total momentum, the most expensive numerical cost comes from the two dimensional integrals, when calculating $\bar{J}(P, t)$ for a range of values of t and P . Very similar integrals must be performed when calculating the T-matrix and the self-energy in the quasi-particle approximation, except that here we have several such integrals. In practice, when starting the iteration from a self-energy obtained in a previous calculation at similar temperature and density, around 10 iteration are sufficient to converge with a relative deviation $\sim 10^{-4}$.

The numerical procedure in its present form introduces a cutoff in momenta of nucleons, to limit the energy range. Thus, we cannot treat more realistic potentials, whose cutoff functions $g(k)$ involve large momenta. On the other hand, with decreasing temperature, the spectral function becomes narrow near the Fermi energy, and cannot be discretized on a finite grid of energy⁷. The extension of the present work to low energies and to large nucleon momenta requires a combined use of quasi-particle approximation near the Fermi energy and for large momenta and a continuum spectral function elsewhere, similar to the ansatz used in Ref. [12].

⁵In the first iteration a constant single-particle width or a stored array of $\text{Im}\Sigma$ obtained earlier for a similar temperature and density is used.

⁶This requires the calculation of the inverse T-matrix for a particular value of momentum and energy (the gap equation) using a procedure to be described later.

⁷The grid must be equally spaced in order to use fast Fourier transform algorithms

References

- [1] D.W. Sprung, in *Advances in Nuclear Physics*, edited by M. Baranger and E. Vogt, (Plenum Press, New York, 1972); C. Mahaux and R. Sartor, in *Advances in Nuclear Physics*, edited by J.W. Negele and E. Vogt, (Plenum Press, New York, 1991)
- [2] A.L. Fetter and J.D. Walecka, *Quantum Theory of Many-Particle Systems* (McGraw-Hill, New York, 1971).
- [3] L.N. Cooper, R.L. Mills and A.M. Sessler, Phys. Rev. **114** (1959) 1377.
- [4] W.H. Dickhoff, Phys. Lett. **B210** (1988) 15; B.E. Vonderfecht, C.C. Gearhart, W.H. Dickhoff, A. Polls and A. Ramos, Phys. Lett. **B253** (1991) 1.
- [5] B.E. Vonderfecht, W.H. Dickhoff, A. Polls and A. Ramos, Nucl. Phys. **A555** (1993) 1.
- [6] B.E. Vonderfecht, W.H. Dickhoff, A. Polls and A. Ramos, Phys. Rev. **C44** (1991) R1265.
- [7] H.S. Köhler, Phys. Rev. **C46** 1687 (1992) 1687.
- [8] T. Alm, G. Röpke, A. Schnell, N.H. Kwong and S. Köhler, Phys. Rev. **C53** (1996) 2181; A. Schnell, T. Alm and G. Röpke, Phys. Lett. **B387** (1996) 443.
- [9] D.J. Thouless, Ann. Phys. (N.Y.) **10** (1960) 553.
- [10] L.P. Kadanoff and P.C. Martin, Phys. Rev. **124** (1961) 670.
- [11] P. Bozek, nucl-th/9811073.
- [12] F. de Jong and H. Lenske, Phys. Rev. **C56** (1997) 154.
- [13] M.I. Haftel and F. Tabakin, Nucl. Phys. **A158** (1970) 1; M. Golberger and K. Watson, *Collision Theory* (John Wiley and Sons, New York, 1964).
- [14] L.P. Kadanoff and G. Baym, *Quantum Statistical Mechanics* (Benjamin, New York, 1962).
- [15] P. Danielewicz, Ann. Phys. **152** (1984) 239.
- [16] W. Botermans and R. Malfliet, Phys. Rep. **198** (1990) 115.
- [17] M. Schmidt, G. Röpke and H. Schulz, Ann. Phys. **202** (1990) 57.
- [18] Y. Yamaguchi, Phys. Rev. **95** (1954) 1628.
- [19] M. Baldo, I. Bombaci, G. Giansiracusa, U. Lombardo, C. Mahaux and R. Sator, Nucl. Phys. **A545** (1992) 741.
- [20] O. Benhar, A. Fabrocini and S. Fantoni, Nucl. Phys. **A550** (1992) 201.
- [21] M. Randeria, N. Trivedi, A. Moreo and T. Scalettar, Phys. Rev. Lett. **69** (1992) 2001; P.G. McQueen, D.W. Hess and J.W. Serene, Phys. Rev. **B 50** (1994) 7304; N. Trivedi and M. Randeria, Phys. Rev. Lett. **75** (1995) 312; R. Micnas, M.H. Pedersen, S. Schafroth, T. Schneider, J.J. Rodríguez-Níñez and H. Beck, Phys. Rev. **B52** (1995) 16223; M.Y. Kagan, R. Frésard, M. Capezzali and H. Beck, Phys. Rev. **B57** (1998) 5995; M. Randeria, cond-mat/9710223
- [22] M.H. Pedersen, J.J. Rodríguez-Níñez, H. Beck, T. Schneider and S. Schafroth, Zeit. für Phys. **B103** (1997) 21.
- [23] J. Maly, B. Jankó and K. Levin, cond-mat/9805018; J. Maly, B. Jankó and K. Levin Phys. Rev. **B56** (1997) R11407; I. Kosztin, Q. Chen, B. Jankó and K. Levin, Phys. Rev. **B58** (1998) R5936.
- [24] Q. Chen, I. Kosztin, B. Jankó and K. Levin, Phys. Rev. Lett. **81** (1998) 4708.
- [25] B. Kyung, E. G. Klepfish and P.E. Kornilovitch, Phys. Rev. Lett. **80** (1998) 3109.
- [26] R. Hausmann, Phys. Rev. **B49** (1994) 12975.

- [27] R. Hausmann, *Zeit. Für Phys.* **B91** (1993) 291.
- [28] A.M. Sessler, in *Liquid Helium*, Proceedings of the International School of Physics Enrico Fermi, edited by G. Careri, (Academic Press, New York, 1963); V.G. Valeev, G.F. Zharkov and Yu.A. Kukharenko, in *Nonequilibrium Superconductivity*, Proceedings of the Lebedev Physics Institute vol. 174, edited by V.L. Ginzburg, (Nova Science Publishers, New York, 1988); D. Rainer and J.A. Sauls, in *Superconductivity*, Lecture Notes of the ICTP Spring College in Condensed Matter on “Superconductivity”, edited by P.N. Butcher and Yu Lu, (World Scientific, Singapore, 1995).
- [29] A.L. Goodman, *Nucl. Phys.* **A186** (1972) 475.
- [30] M. Baldo, U. Lombardo and P. Schuck, *Phys. Rev.* **C52** (1995) 975.
- [31] A.B. Migdal, *Theory of Finite Fermi Systems* (John Wiley and Sons, New York, 1967).
- [32] J.R. Schrieffer, *Theory of Superconductivity* (W.A. Benjamin, Inc., Massachusetts, 1964); G.D. Mahan, *Many-Particle Physics* (Plenum Press, New York, 1981).
- [33] P.W. Anderson and P. Morel, *Phys. Rev.* **123** (1960) 1911.
- [34] R. Balian and N.R. Werthamer, *Phys. Rev.* **131** (1963) 1553.
- [35] P.W. Anderson and W.F. Brinkman, in *The Physics of Liquid and Solid Helium, part II*, edited by K.H. Benneman and J.B. Ketterson, (John Wiley and Sons, New York, 1978).
- [36] A.D. Jackson, A. Lande and R.A. Smith, *Phys. Rep.* **86** (1982) 55.